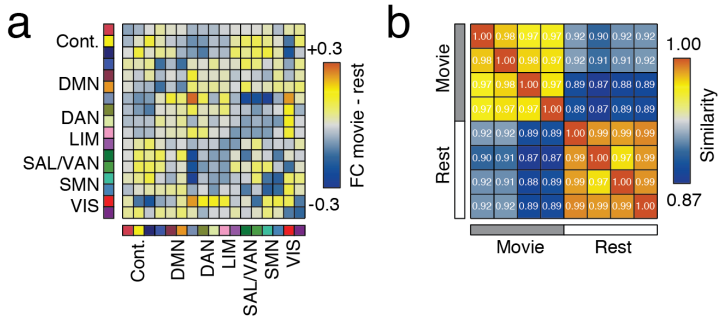

FIG. S1. **Comparison of time-averaged FC.** (*a*) Difference in system- and time-averaged FC between movie and resting conditions. (*b*) Mean similarity of time-averaged movie and resting FC.

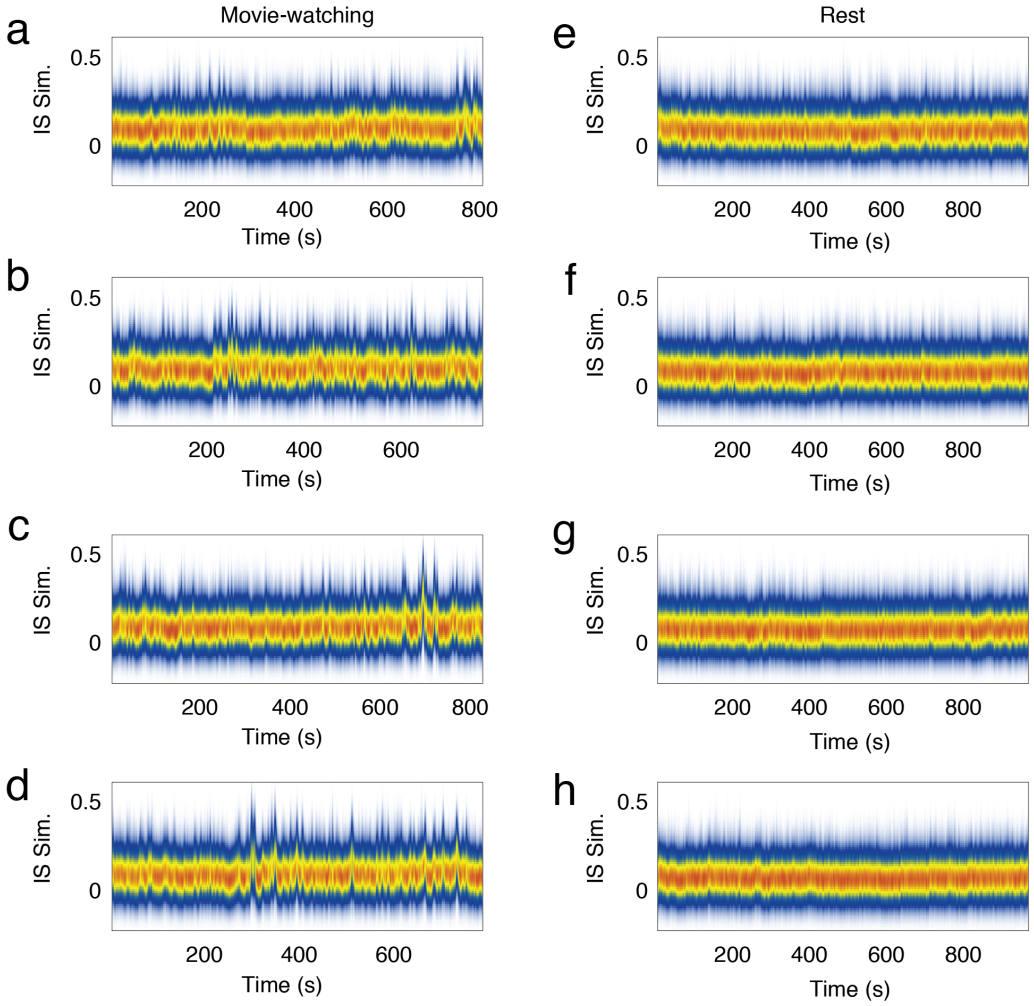

FIG. S2. **Inter-subject similarity distributions.** Panels *a*-*d* depict ISS distributions across time for all four movie-watching scans. Panels *e*-*h*, on the other hand, depict ISS distributions at rest.

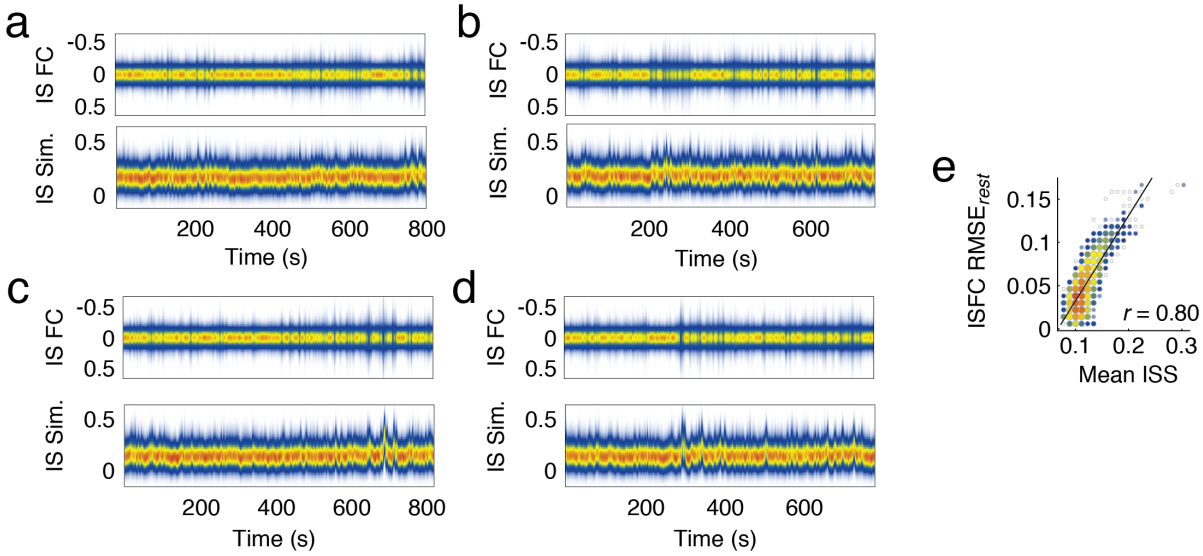

FIG. S3. **Comparison of inter-subject similarity and inter-subject FC.** In the main text, we focus on the measure of inter-subject similarity (ISS). It involves estimating time-varying networks for every individual assessing their similarity at each time point. This approach enables us to identify points in time when network architecture is share across individuals while simultaneously modeling every individual's whole-brain network, which further allows us to estimate measures like network modularity. An alternative approach for identifying shared network structure involves estimating time-varying inter-subject FC (ISFC), or the correlation of activity in region i in subject s with region j in subject t and repeating this procedure for all pairs of regions, all pairs of subjects, and at every time point [46]. Here, in panels a - d, we show distributions of ISFC alongside ISS. We note that, in general, periods of high ISS coincide with periods of strong (positive or negative) ISFC. In panel e we quantify this relationship by computing the correlation between mean ISS and the difference between the ISFC distribution during movie watching compared to rest (root mean squared-error). This indicates that ISS and ISFC, while they relate subjects' networks to one another differently, identify similarity across subjects at roughly the same points in time.

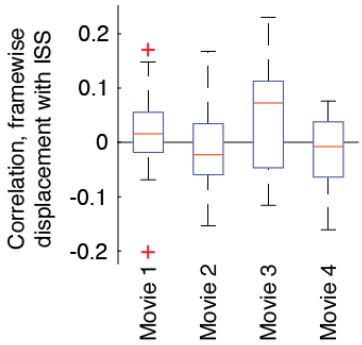

FIG. S4. **Correlation of in-scanner head motion with inter-subject similarity.** We calculated the mean framewise displacement (FD) for each subject within each window (10 TRs or approximately 8.13 s). To assess whether motion might be related to ISS, we calculated the Pearson correlation of each subject's FD with mean inter-subject similarity (ISS). In general, we found that correlations were consistently centered around to zero for all four movies, suggesting that ISS is not obviously driven by in-scanner motion.

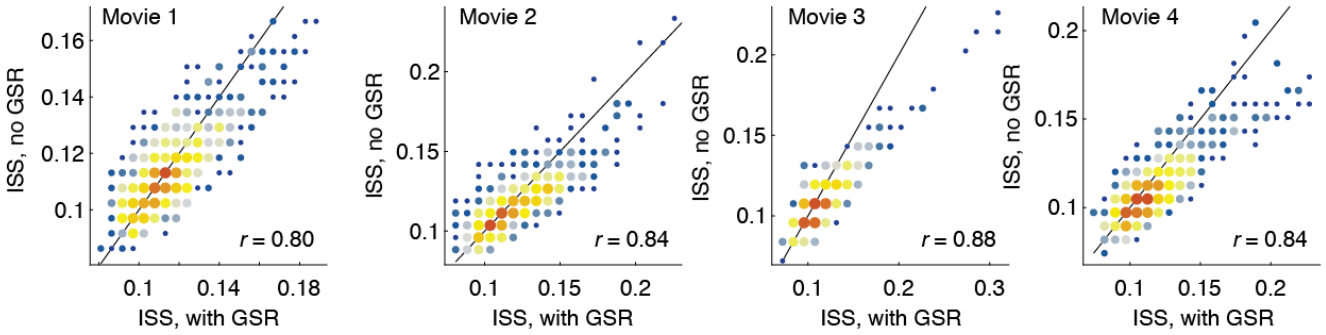

FIG. S5. **Effect of global signal regression on mean inter-subject similarity for the four movie scans.** We calculated inter-subject similarity using data that was processed identically to the what was described in the main text. The only processing step that was omit was the regression of mean gray matter BOLD signal from the data. Here, we compare those ISS measures (labeled ISS, no GSR) wit the ISS measures from the main text (ISS, with GSR). We find that the two are highly correlated, suggesting global signal regression has little effect on ISS.

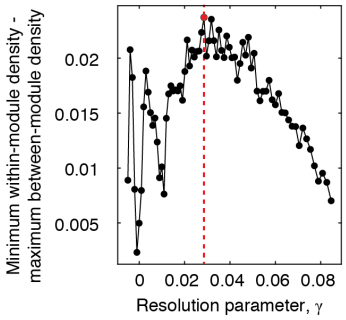

FIG. S6. **Choice of optimal resolution parameter for edge clustering.** The community detection algorithm used to partition edges into communities depends on a resolution parameter, γ, whose value determines the size/number of detected communities. We selected γ such that the partitions detected at that value produced communities that were maximally segregation. That is, when the minimum internal density of connections across all communities minus the maximum density of connections across communities achieved its peak.

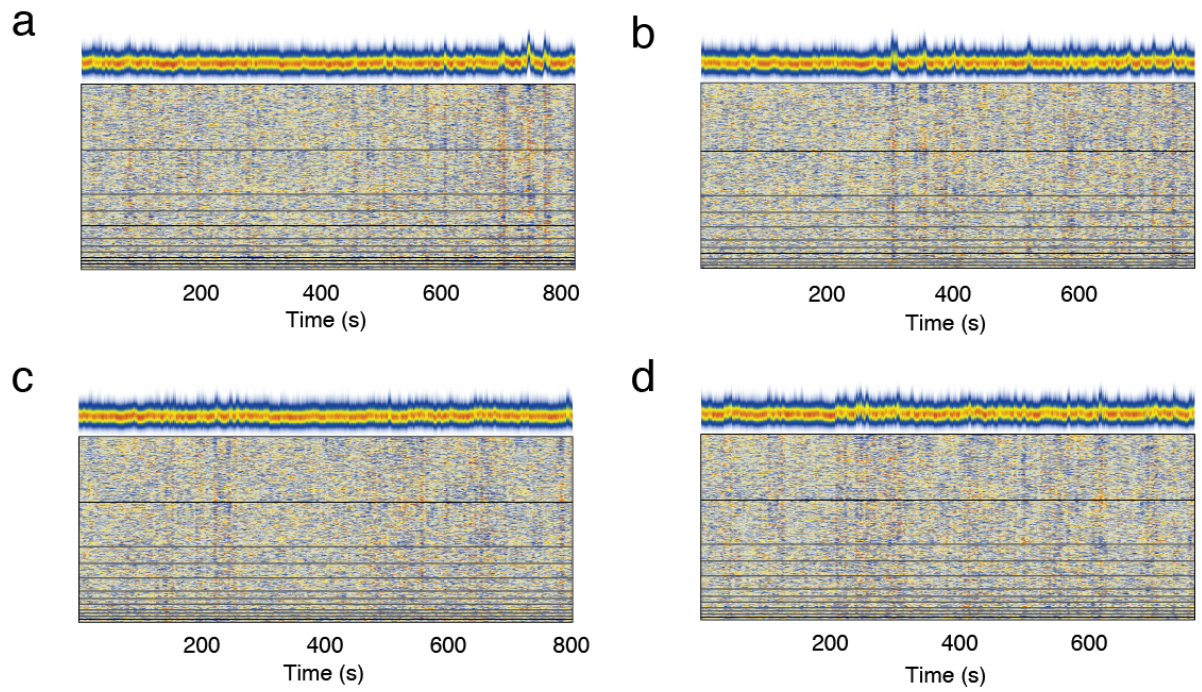

FIG. S7. **Edge trajectories ordered by community.** Panels *a*-*d* depict edge trajectories ordered by community for all four movies.

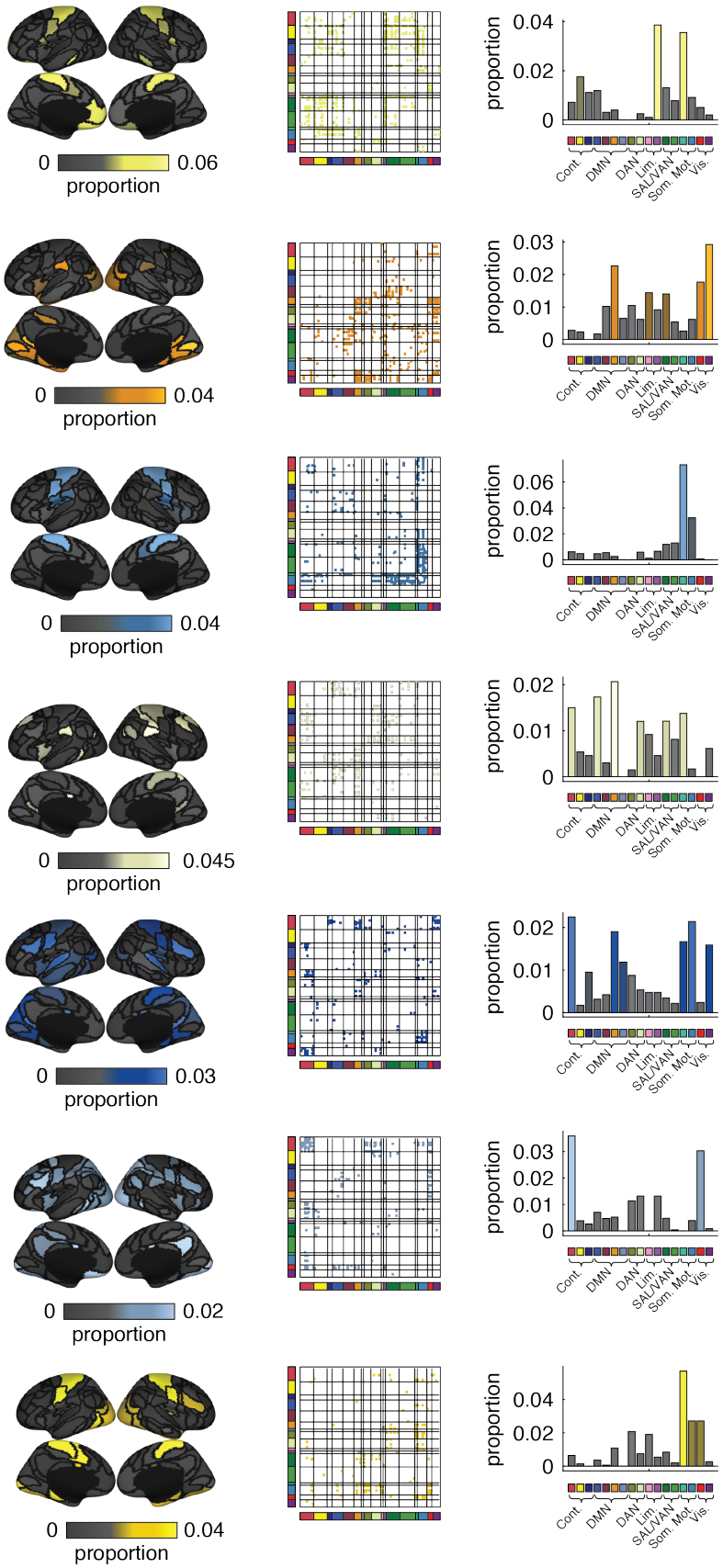

FIG. S8. **Remaining edge communities.** In the main text we showed the five largest edge communities. We show the remaining seven here.

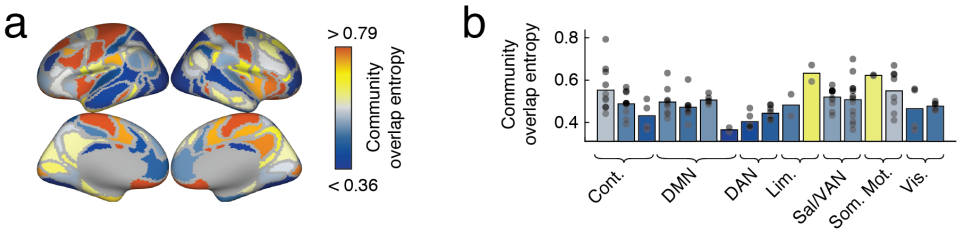

FIG. S9. **Edge community overlap.** For each node we calculated the entropy of its edges' community assignments. Small values indicate that those edges tended to be assigned to a small subset of communities, while larger values indicate a broader distribution of community labels. In panel *a* we show the entropy values distributed over cortex, while in panel *b* we show those same values aggregated by system.

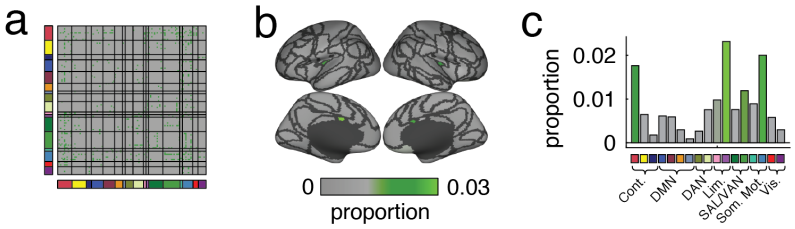

FIG. S10. **Small and singleton communities.** In the main text we clustered edge correlation matrices so that every edge was associated with a community label. We reported the twelve largest communities, however there were many small communities comprised of only a few edges. Here, we aggregate those communities into a single label and provide a short summary of their properties. (*a*) Edges assigned to these communities. (*b*) Projection of those connections onto brain areas. (*c*) Those projections averaged according to brain system.

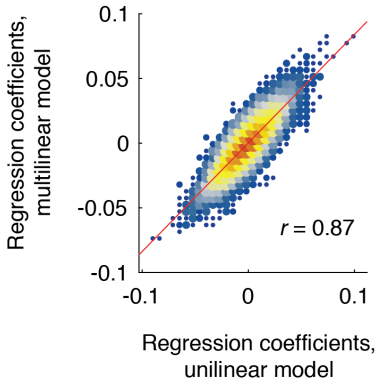

FIG. S11. **Comparison of regression coefficients estimated using uni-/multi-linear modeling.** In the main text we reported β coefficients estimated from linear models of the form $\hat{y} = \beta_0 + \beta_1 x_1 + \epsilon$. Here, we compare them against multi-linear models in which we allow many predictors to compete for the same variance. These models have the form $\hat{y} = \beta_0 + \sum_i \beta_i x_i + \epsilon$. As means of comparison, we aggregated into a vector the coefficients for a given predictor (movie feature) for all connections. We repeated this procedure for both the uni-linear and multi-linear models and computed the correlation of those two vectors. In general, we find excellent correspondence. When all features are combined, we obtain a correlation of $r = 0.87$. Individually, there was more variability across predictors, but still with excellent correspondence, with mean $\pm$ standard deviation correlations of $r = 0.88 \pm 0.08$.

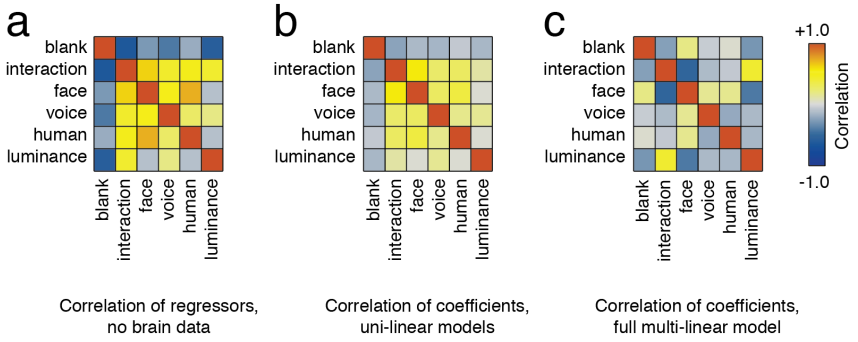

FIG. S12. **Impact of correlated regressors.** In the main text we reported β coefficients estimated from uni-linear models of the form $\hat{y} = \beta_0 + \beta_1 x_1 + \epsilon$. In Fig. S11, we compared them against multi-linear models in which we allow many predictors to compete for the same variance. Here, we show the correlation structure of β coefficients for both models alongside the correlation structure of the regressors, corresponding to a blank screen, an interaction between humans, presence of a face, voice, presence of a human, or baseline fluctuations in luminance. In general, we find that the regression structure of uni-linear models closely matches that of the regressors, themselves ($r = 0.95$). The multi-linear model, on the other hand, allows regressors to compete for the same variance, and as a result exhibits correlation structure dissimilar from the regressors on their own ($r = -0.06$). We note, however, that the β coefficients from both the uni-linear and multi-linear models are, nonetheless, highly correlated (See Fig. S11).

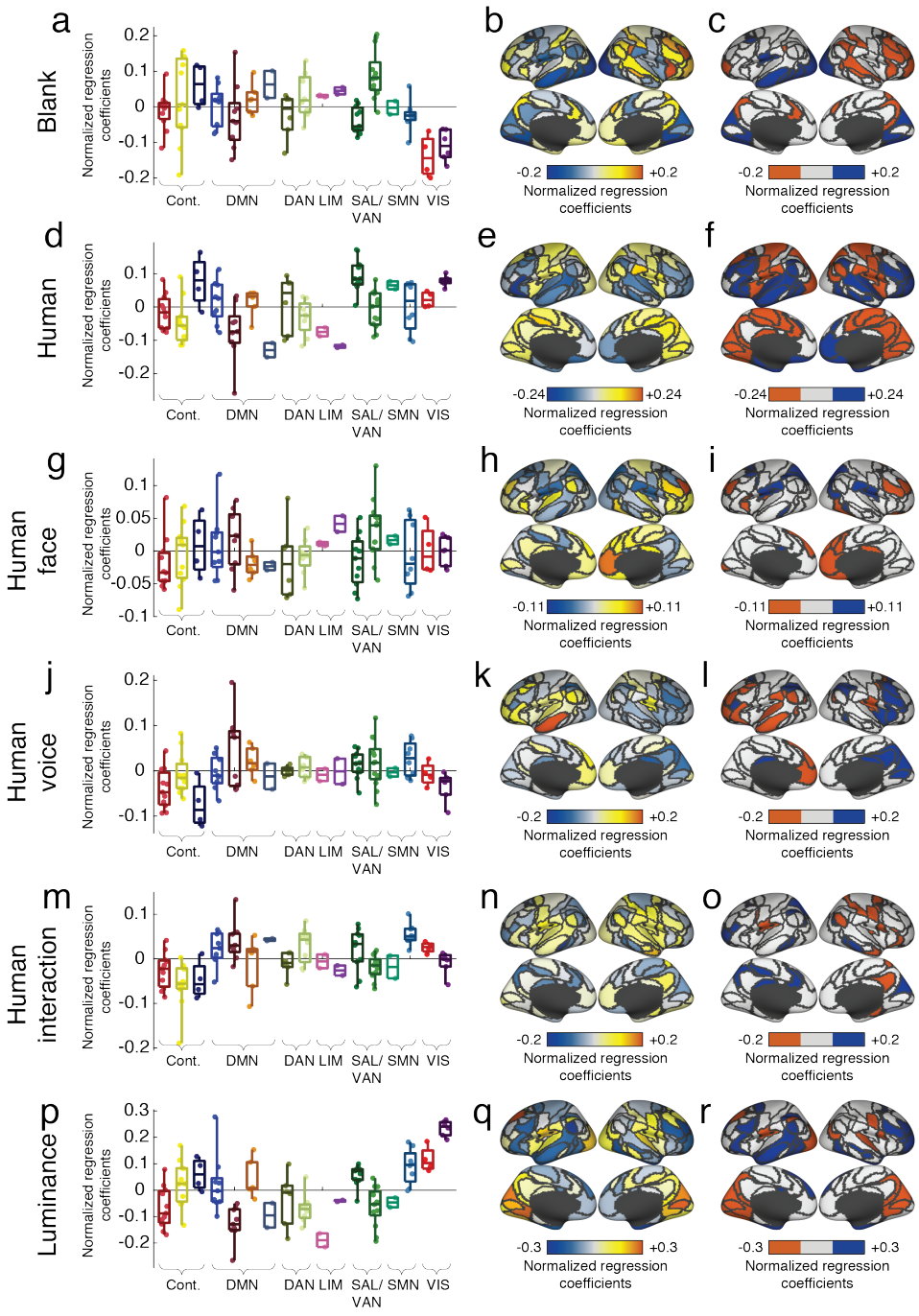

FIG. S13. **Associations between regional participation coefficient and movie features.** We calculated regional participation coefficients (PC) for every subject and brain region and for all movies and at every time point. We z-scored PCs within each movie and subject, averaged these values across subjects, and further concatenated PC values over all four movies. We then used the same multi-linear modeling framework described in the main text to test for associations of PC with movie features. In general, we found significant correlations at the regional level for all six features. Every row in this panel summarizes results from a specific feature. For example, the first row corresponds to regions whose participation coefficient was associated with the appearance of blank screens. In panel *a*, we show normalized regression coefficients grouped according to brain systems. In panel *b*, we show the same regression coefficients projected back onto the cortical surface and in panel *c*, we show the results of imposing a statistical threshold on the coefficients (p-value selected to maintain an false discovery rate of no greater than 5%). Subsequent rows show analogous plots for the remaining features.

Scan	**Title**	**Genre**	**Runtime**
1	Man Up and Go	documentary/emotional	4m20s
1	The First 70	documentary	3m
1	Fixation	documentary/adventure	1m42s
1	The Living	drama	2m
1	SAMSARA	documentary/“unparalleled sensory experience”	1m35s
1	Blood Brother	documentary	2m20s
2	Birdmen	documentary/adventure	3m59s
2	Groomed	drama	1m30s
2	Cold	outdoor/sports	2m
2	Sleepwalkers	drama	2m
2	A Kind of Show	comedy	1m
3	Geofish	documentary/adventure	4m40s
3	The Debut	outdoor/sports	3m23s
3	Dreams of a Life	documentary/mystery	2m10s
3	The Front Man	documentary	2m30s
3	This Is Vanity	drama	1m
4	Planetary	documentary	4m30s
4	Sign Painters	documentary	2m50s
4	Florida Man	documentary/drama	2m
4	The Sleeping Bear	drama	3m40

TABLE S1. **Movies included in each movie scan.**